Supporting Information
The inert pair effect on the heavy noble gases: New insights from radon tetroxide.

Nuno A. G. Bandeira*[1], Joaquim Marçalo[2]

[1] BioISI, Faculdade de Ciências, Universidade de Lisboa, Campo Grande, 1749-016 Lisboa, Portugal.
[2] Centro de Química Estrutural, Institute of Molecular Sciences, Instituto Superior Técnico, Universidade de Lisboa, Estrada Nacional 10, 2695-066 Bobadela LRS, Portugal.
*Email: nuno.bandeira@ciencias.ulisboa.pt

Contents

1. Radial structures of relativistic and non-relativistic atoms at the Hartree-Fock level

Table S 1 – Radial expectation values of Ng atoms and Ng^{8+} ions, with and without relativity.

HF/x2c-TZVPP	$\langle r_{ns} \rangle$/a.u.	$\Delta\langle r_{ns} \rangle$/a.u.	$\langle r_{np} \rangle$/a.u.	$\Delta\langle r_{np} \rangle$/a.u.
Xe	1.903	-0.111	2.320	-0.025
nr-Xe	2.014		2.345	
Xe^{8+}	1.645	-0.060	1.822	-0.030
nr-Xe^{8+}	1.705		1.852	
Rn	1.923	-0.368	2.463	-0.191
nr-Rn	2.291		2.654	
Rn^{8+}	1.679	-0.287	1.948	-0.219
nr-Rn^{8+}	1.966		2.167	

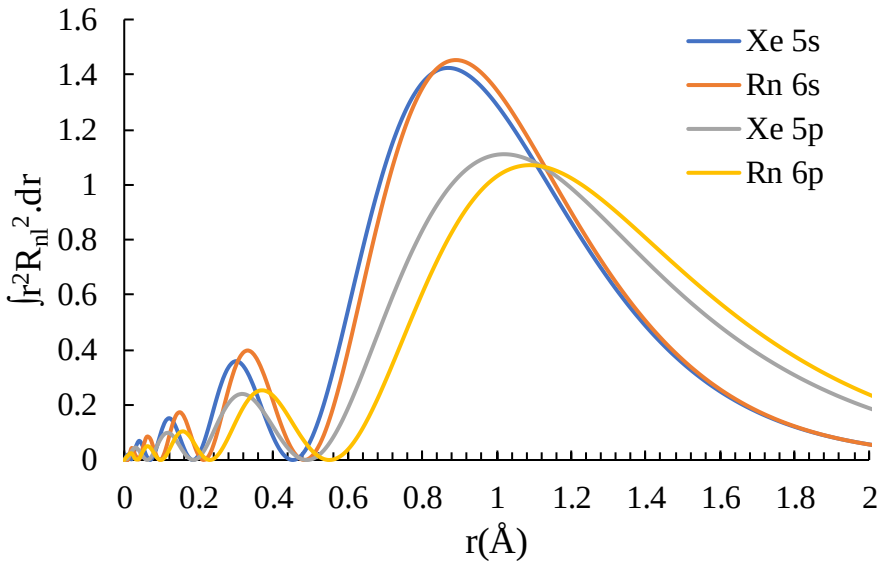

Figure S 1 – Electronic radial distribution densities of the s and p shells of Xe and Rn atoms at the HF/def2-TZVPP level.

2. Structure and Bonding of NgO_4.

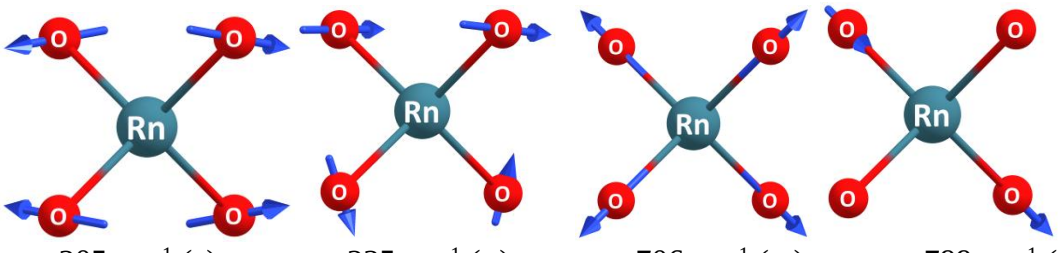

205 cm^{-1} (e) 225 cm^{-1} (t_2) 706 cm^{-1} (a_1) 799 cm^{-1} (t_2)

Figure S 2 – Vibrational modes of radon tetroxide calculated with CCSD(T)/DKH-TZVPP. Blue arrows show the atomic displacements.

3. Structure and Bonding of $Ng(\eta^2\text{-}O_2)_2$.

A CASPT2(22,15) optimisation was performed explicitly correlating all the p orbitals in Ng and O. The result was the maintaining of D_{2h} symmetry with a O-O bond length of 1.447 Å (Figure S 3).

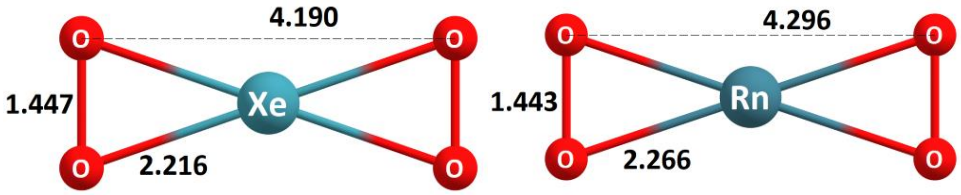

Figure S 3– Optimised CASPT2(22,15) molecular structure of $Ng(\eta^2\text{-}O_2)_2$ (Ng=Xe,Rn) with selected bond distances (Å).

The ground state electronic structure is constituted of a two configurational wavefunction by the interaction of a set of π* orbitals from the di-oxo ligands (Figure S 4). The leading configuration is 61.3% of the total wavefunction and the remainder 16.7% corresponds to the doubly occupied in phase π* fragment MOs (Figure S 4 and Table S 2).

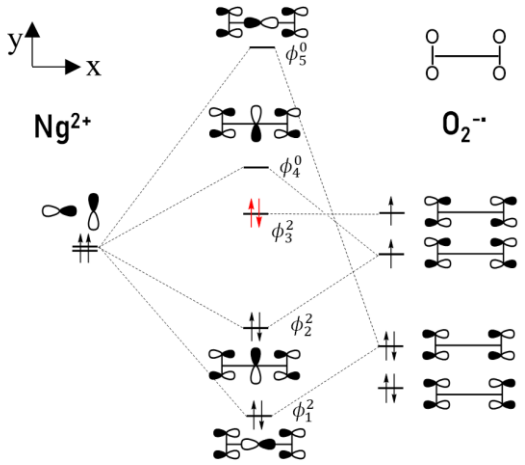

Figure S 4 – Principal orbital interactions and dominant electron configuration in $Ng(\eta^2\text{-}O_2)_2$ species. The remaining valence orbitals that are not shown are all doubly occupied.

Table S 2 – Squared amplitudes (×100) of each CASSCF(22,15) configuration state function.

CSF	$Xe(\eta^2\text{-}O_2)_2$	$Rn(\eta^2\text{-}O_2)_2$
$\lvert\phi_1^2\phi_2^2\phi_3^2\phi_4^0\phi_5^0\rangle$	61.3	60.9
$\lvert\phi_1^2\phi_2^2\phi_3^0\phi_4^2\phi_5^0\rangle$	16.7	19.5

Furthermore, this configurational admixing may be quantified via the non-adiabatic coupling matrix elements obtained from the effective Hamiltonian pursuant to

a Mk(2,2)-CCSD(T)/x2c-TZVPP//CASPT2(22,15)/x2c-TZVPP calculation. The main parameters are summarised in Table S 3.

Table S 3 – Properties of the two configurational mixing of the ground state of $Ng(\eta^2\text{-}O_2)_2$ species.

Mk(2,2)-CCSD(T)	Adiabatic GS c_μ **$Xe(\eta^2\text{-}O_2)_2$**	**ΔE_{adiab} (a.u.) $Xe(\eta^2\text{-}O_2)_2$**	**ΔE_{diab} (a.u.) $Xe(\eta^2\text{-}O_2)_2$**	Adiabatic GS c_μ **$Rn(\eta^2\text{-}O_2)_2$**	**ΔE_{adiab} (a.u.) $Rn(\eta^2\text{-}O_2)_2$**	**ΔE_{diab} (a.u.) $Rn(\eta^2\text{-}O_2)_2$**
1: $\left\|\phi_1^2\phi_2^2\phi_3^2\phi_4^0\phi_5^0\right\rangle$	-0.890	0	0	-0.886	0	0
2: $\left\|\phi_1^2\phi_2^2\phi_3^0\phi_4^2\phi_5^0\right\rangle$	0.456	+0.2812	+0.1587	0.464	+0.2748	+0.1480
H_{12} (a.u.)			+0.1128			+0.1121
H_{21} (a.u.)			+0.1194			+0.1196

The p_z orbital sets in the O_2^- fragment are all doubly occupied and so do not count to the overall bond making process as their bonding and antibonding counterparts are completely filled. The CASPT2 natural orbital occupations (Figure S4 and Table S 4) allow for the extraction of bond parameters such as the Effective Bond Order.[1]

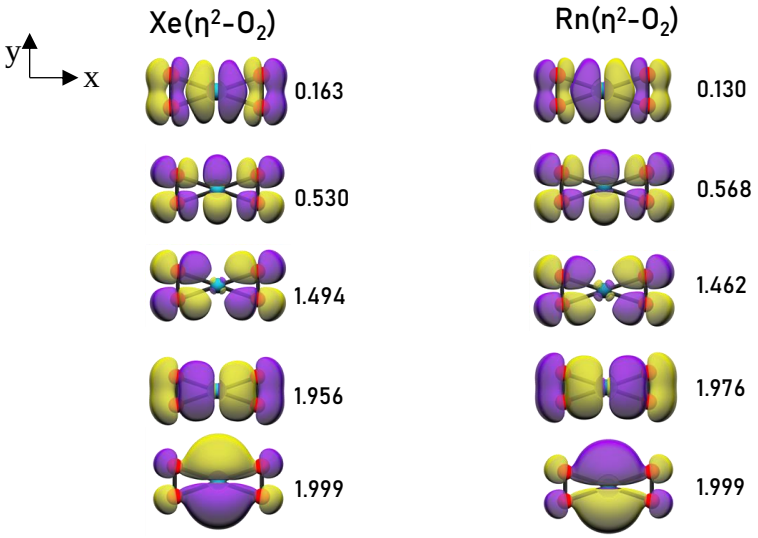

Figure S 5 – CASPT2(22,15) Natural Orbital Occupations for the most important frontier orbitals (as shown in Figure S 4) in $Ng(\eta^2\text{-}O_2)_2$.

In addition, the CASPT2 natural orbitals may undergo localisation by feeding the Pt2Orb file into the *&LOCALISATION* module to extract individual atomic occupations from the localised natural orbitals (LNO). It may be seen that both $Xe(\eta^2\text{-}O_2)_2$ and $Rn(\eta^2\text{-}O_2)_2$ have very similar bonding features.

Table S 4 – Essential localised natural occupancies obtained from CASPT2(22,15)/x2c-TZVPP level natural orbitals.

CASPT2 LNO populations	**$Xe(\eta^2\text{-}O_2)_2$**	**$Rn(\eta^2\text{-}O_2)_2$**
Ng p_y	1.82	1.82
Ng p_x	1.01	0.916
Ng p_z	1.97	1.97
$O_2^{\bullet-}$ (π^*_x)	1.09 (×2)	1.09 (×2)
$O_2^{\bullet-}$ (π_x)	1.47 (×2)	1.52 (×2)

$O_2^{\bullet-}$ (π^*_z)	1.97 (×2)	1.97 (×2)
$O_2^{\bullet-}$ (π_z)	1.98 (×2)	1.98 (×2)
$O_2^{\bullet-}$ (σ^*_y)	0.084 (×2)	0.083 (×2)
$O_2^{\bullet-}$ (σ_y)	1.91 (×2)	1.91 (×2)
Effective Bond Orders		
Ng-O	0.45	0.42
O-O	1.11	1.13

Analysis of the vibrational modes calculated numerically with CASPT2 confirms the stationary point as a local minimum (Figure S 6, Table S 5). The smallest vibrational displacement corresponds to an in-plane rotation of the superoxo- groups (36 and 13 cm^{-1}). The three vibrational modes revealing the Rn-OO bond strengths show up in the 300 cm^{-1} range. These are consistently more energetic than the corresponding Xe-OO vibrations by a few dozen cm^{-1}.

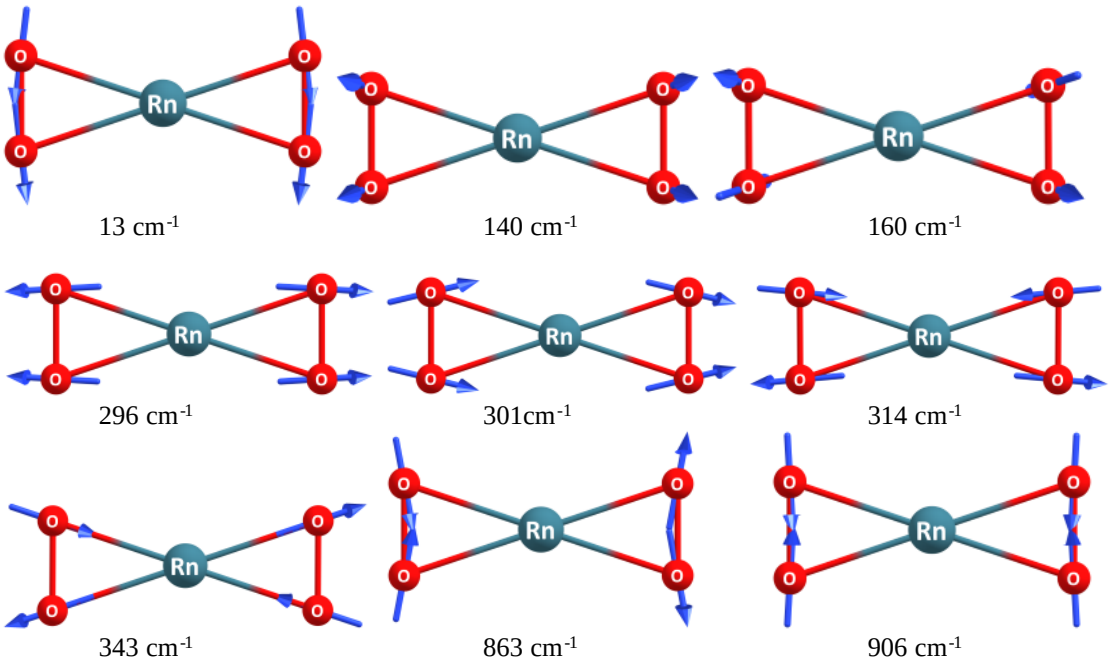

Figure S 6– CASPT2(22,15) vibrational modes of $Rn(\eta^2\text{-}O_2)_2$. See Table S 5 for intensities.

Table S 5 – CASPT2(22,15)/x2c-TZVPP vibrational modes of $Ng(\eta^2\text{-}O_2)$.

Modes	**ν/cm^{-1} $Xe(\eta^2\text{-}O_2)_2$**	**Int.**	**ν/cm^{-1} $Rn(\eta^2\text{-}O_2)_2$**	**Int.**
1	36	13.2	13	14.3
2	171	11.1	140	11.3
3	196	0.025	160	4.94
4	265	6.2×10^{-4}	296	2.61×10^{-3}

5	283	45.1	301	38.6
6	295	0.019	314	6.02
7	308	6.3	343	1.69×10^{-4}
8	844	25.9	863	37.7
9	902	3.4×10^{-3}	906	3.6×10^{-4}

4. Structure and Bonding in $NgO_2(\eta^2\text{-}O_2)$.

The $NgO_2(\eta^2\text{-}O_2)$ geometry (Figure S 7) was likewise optimised using the CCSD(T)/DKH-TZVPP protocol. The structure where the peroxide group is in the same plane as the two oxygen atoms is actually a transition state leading to the presently obtained local minimum. The structure with the peroxide group exactly perpendicular to the two oxygen atoms is not even a stationary point and will also lead to the presently obtained local minimum.

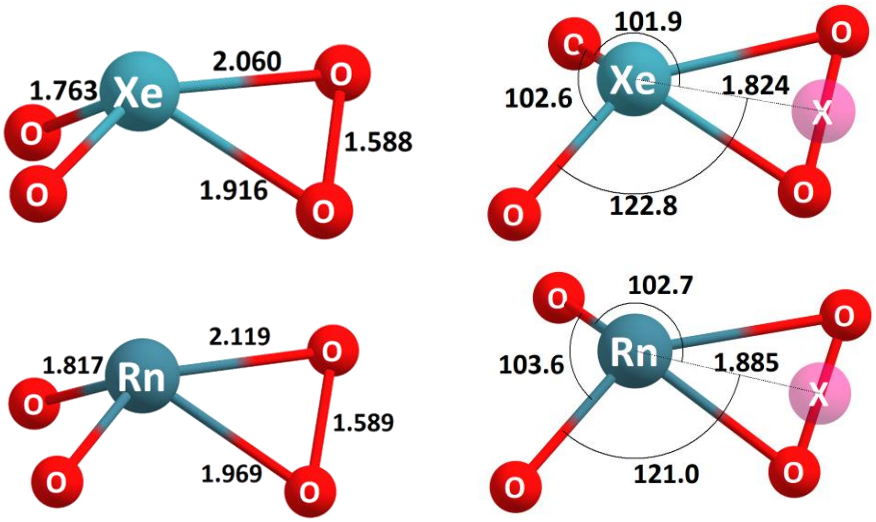

Figure S 7 – CCSD(T)/DKH-TZVPP optimised structures of $NgO_2(\eta^2\text{-}O_2)$ with distances (left) in Å and angles (right) in degrees.

An NBO analysis was performed on the obtained minimum and a natural Lewis structure can be assigned with a conventional electron pair bond on Ng-O^1 and a more charge polarised donating Ng←O^2 bond (Figure S 8). The Mayer-Mulliken bond orders (MBO) confirm the asymmetry of these bonds: Xe-O^1= 0.913, Xe-O^2=0.637; Rn-O^1=0.718, Rn-O^2=0.540.

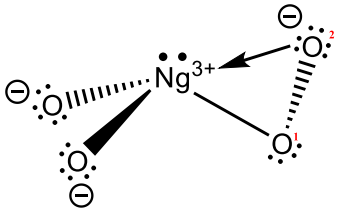

Figure S 8 – Natural Lewis structure of $NgO_2(\eta^2\text{-}O_2)$ with formal charges.

Table S 6 – Natural Bond Orbital analysis of the $NgO_2(\eta^2\text{-}O_2)$ species performed at the CCSD/DKH-TZVPP level.

Natural Populations	**$XeO_2(\eta^2\text{-}O_2)$**	**$RnO_2(\eta^2\text{-}O_2)$**
NAO Ng 5s/6s	1.707	1.780
NAO Ng 5p/6p	3.328	3.109
NLMO composition		
σ(Ng-O[1])	38.3% Xe + 61.7% O	36.0% Rn + 64.0% O
σ(Ng-O[2])	14.1% Xe + 85.9% O	11.7% Rn + 88.3% O

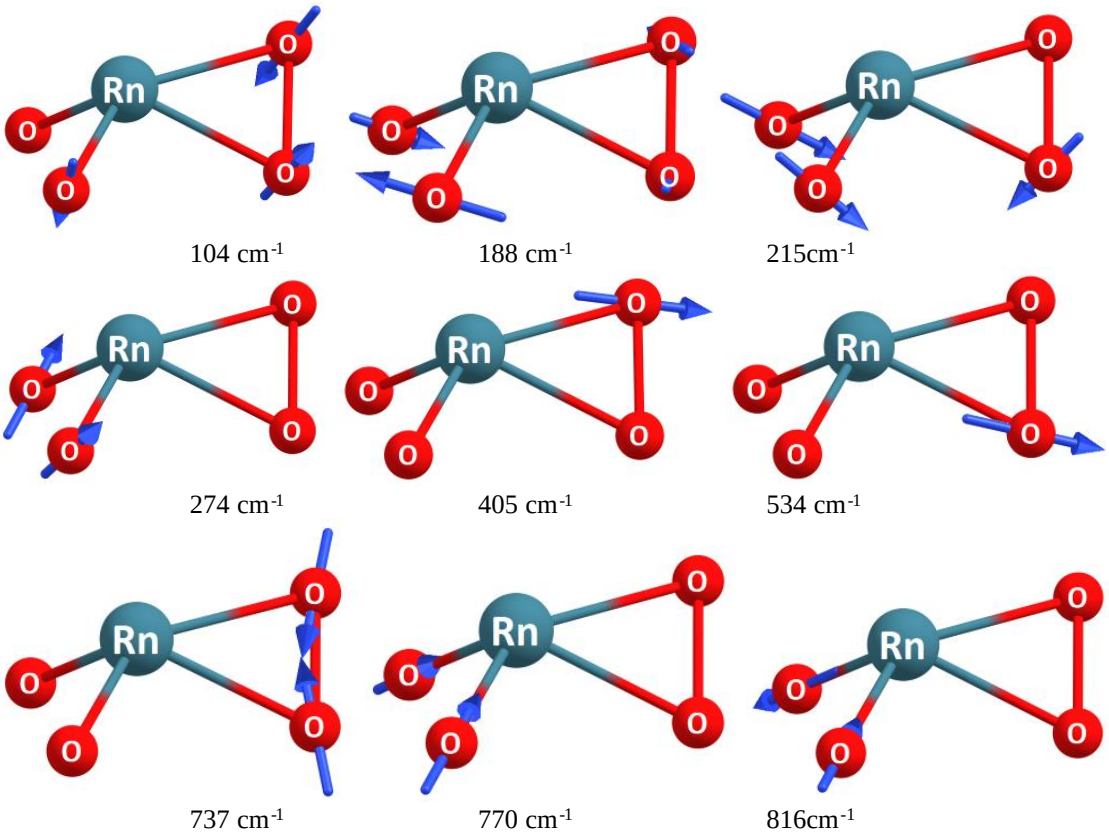

Figure S 9 - Vibrational modes of radon di-oxo peroxide calculated with CCSD(T)/DKH-TZVPP.

Table S 7 – Comparison between the vibrational modes of $NgO_2(\eta^2\text{-}O_2)$ calculated at the CCSD(T)/DKH-TZVPP level.

Modes	**ν/cm^{-1} $XeO_2(\eta^2\text{-}O_2)$**	**Int.**	**ν/cm^{-1} $RnO_2(\eta^2\text{-}O_2)$**	**Int.**
1	133	2.48	104	4.29
2	223	11.8	188	9.78
3	276	18.7	215	18.0
4	327	13.3	274	12.3
5	443	66.3	405	57.6

6	565	27.2	534	22.4
7	750	2.54	737	2.63
8	823	60.2	770	51.2
9	864	79.0	816	67.2

1. Roos BO, Borin AC, Gagliardi L. Reaching the Maximum Multiplicity of the Covalent Chemical Bond. *Angew Chem Int Ed* 2007, **46**(9)**:** 1469-1472.